Micro-arc Tests for MHD electrode materials

Hideaki USAMI, Ryo NISHIMURA, Yoshiaki AOKI,
Naoyuki KAYUKAWA and Takayasu OKUO+

(Received August 19, 1993)

Abstract

Improving the durability of the anode electrode for the coal-fired MHD channel is an important research subject.

This paper describes the results of the micro-arc tests (the power arc tests) for 21 metallic and 4 ceramic electrode materials. Their arc resistances were specified by the observation of the crater formed by pulse current applied. Also described are the results of the splash experiments (the power arc tests is carried out under coal-fired MHD simulation) for TiC-coated stainless steel (TiC/SUS) electrodes.

The results of micro-arc tests indicate that tungsten, tungsten-based alloy, tantalum, molybdenum, platinum and TiC-coated stainless steel have the desirable arc resistances.

In the splash experiment, TiC-coated stainless steel electrode has more desirable arc resistance than the electrode without TiC layer.

1. Introduction

In an open cycle MHD generator channel, a micro-arc discharge is observed when cold-type slagging electrode is used for an anode (cold-type slagging anode). This discharge occurs in a particular condition of little wettability between the electrode and the slag and a decrease of the slag layer thickness during the electric current flows. Under this condition average current density of microarc discharge is usually 0.3~0.35 A/cm^2,[1] and many arc spots having a life of less than 30 ms appear. Such discharge condition is easily simulated by applying a pulse current.

This paper is a technical report which describes the experimental results of arc-resistance characteristics of electrode materials. These materials were selected from various pure metals and refractory alloy which are used for electrode of an MHD generator and the first wall of a nuclear fusion reactor. Their arc resistances were specified by the observation of the crater-formation properties. This specification was carried out by applying a strong heat impact (1 A-2~8 ms pulse current) on the surface of the material. Also described are the 1.5 MWth COM combustion splash experiments which were carried out to determine MHD electrode materials having desirable arc resistance under the slagging conditions.

2. Basic Discharge Experiment to Evaluate the Arc Resistance.

In an open cycle MHD generator channel, cold-type electrodes with a slag layer

+ Electrotechnical Laboratory, 1-1-4 Umezono, Tsukuba-shi Ibaraki 305, Japan

should be adopted. They are forced to be cooled in order to erase the Joule heating and realize their long lifetime. On these electrodes, the current flows in arc-discharge mode and dominates the electrode wear. This arc-discharge current has the enormously high discharge energy, i. e. high heat flux (~300 W/cm²) and current density (~1 A/cm²). The similar discharge characteristics is obtained when a discharge occurs between the narrow electrode gap (≦1 mm). Therefore, we evaluated the arc resistance of high-meltingpoint materials by applying the energy of this narrow-electrode-

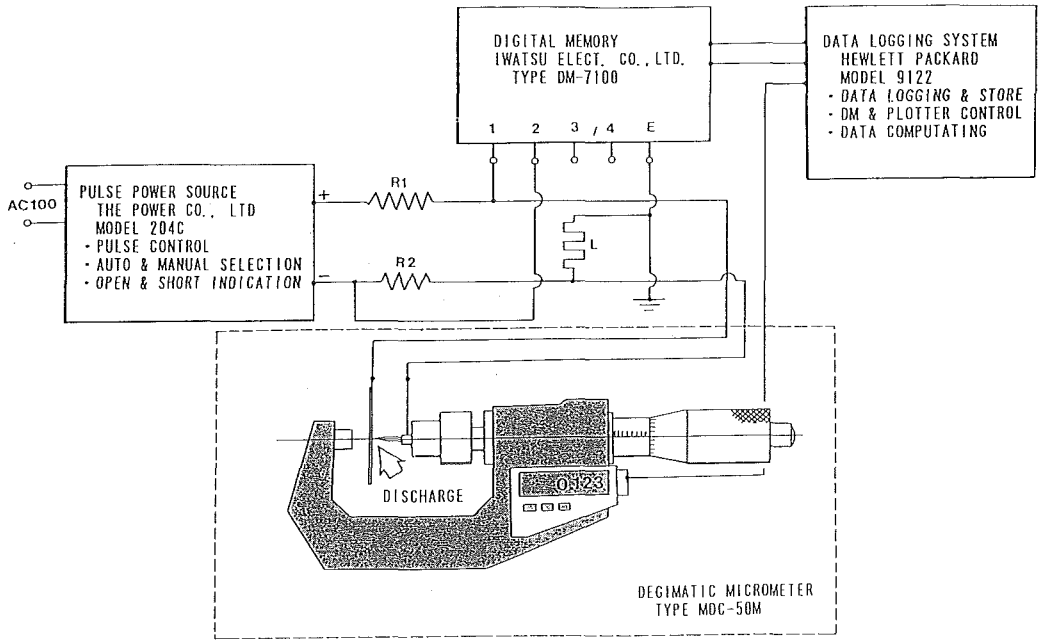

Fig. 1 The block diagram of the -arc discharge electrode testing system.

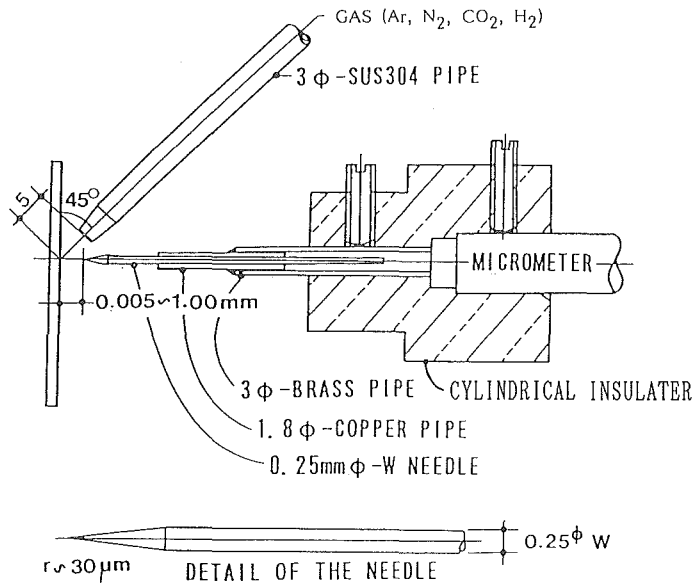

Fig. 2 Electrodes for the microarc discharge experiment.

gap discharge.

2. 1 Experimental apparatus

Figure 1 shows the experimental arrangement used to occur arc discharge between micro gap. It is composed of a discharge-gap-control instrument, a pulse power source, a wave analyzer of voltage and current, and a data processor. The discharge-gap-control instrument adjusts the gap length of the discharge part of the pair of needle- and plate- electrodes by a digital micrometer. The pulse power source can supply rectangular-shaped constant current pulses singly or continuously to the gap. The wave shapes of the pulse-voltage and -current fed into the discharge gap are accumulated temporarily in a digital memory at every 5 μs intervals. The data processor calculates and transforms the voltage and current data collected in the digital memory into the amount of energy. Then the characteristics of the time dependence of voltage and current are made to be individual wave information.

This system can precisely evaluate the pulse energy, even if it shows complicated waveforms including much noise. This system also has the advantage that it can measure and compare the discharge phenomena and the waveform of the voltage and current at almost the same time.

Figure 2 shows the composition of a pair of needle- and plate- electrodes for the microarc experimental equipment shown in Fig. 1. A needle-electrode is a tungsten needle and fixed to the central axis of a cylindrical insulator. The insulator is fixed to a spindle of a micrometer. The radius of curvature of the point of the needle electrode is 25~30 μm. The plate-electrode, which is made of the material to be tested, is placed perpendicularly to the central axis of the needle-electrode. The gap length is set at 0.005~2.00 mm. During the discharge experiment the environment control gas (e. g. Ar, N_2, CO_2, dry air) of 50 cm^3/min is blown into the discharge gap.

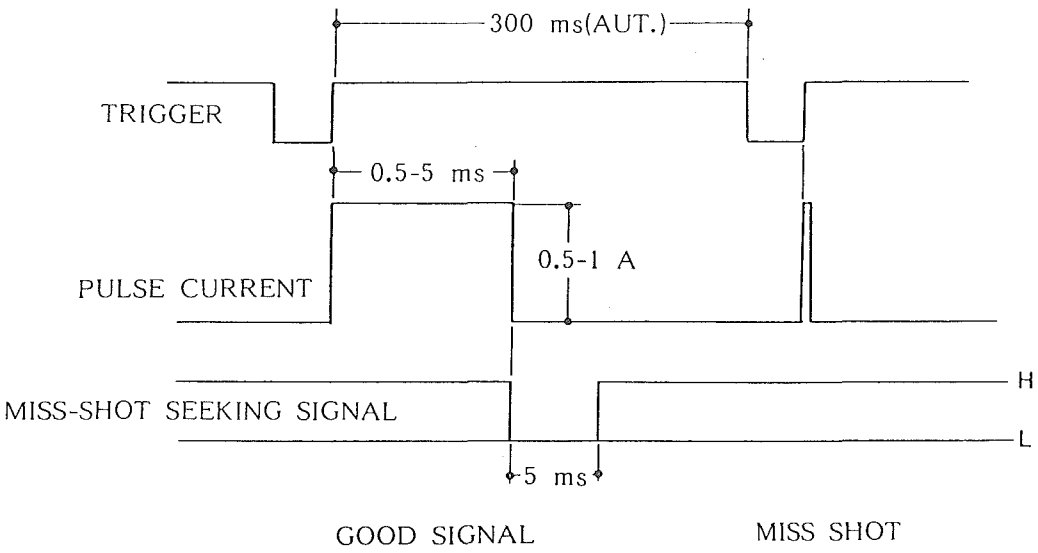

Fig. 3 Pulse current shape applied to the micro-arc discharge experiment.

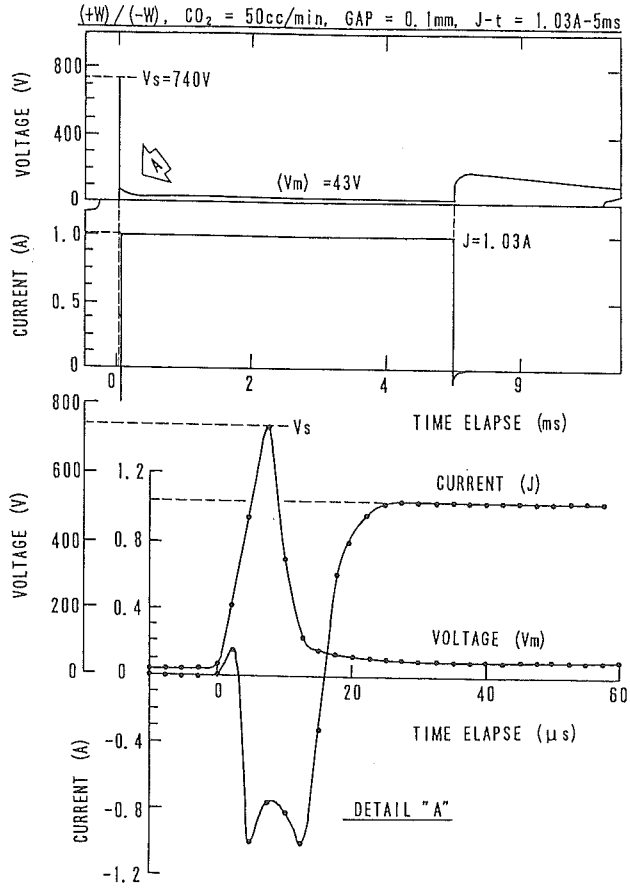

Fig. 4 An example of voltage and current observed between a tungsten needle-anode and a tungsten plate-cathode in a CO_2 gas atmosphere.

Figure 3 shows the time chart of the pulse current. The practical value of the current pulse range is 0.5~1 A/0.5~5 ms, and the trigger of the pulse is arbitrarily selected manually or automatically. When the automatic trigger is selected, it is possible to feed continuous pulses at 300 ms intervals. The shot number is counted and memorized for the proper pulse. The miss-shot judgment circuit counts miss-shot signals in cases of the occurrence of miss shots, of which pulse energy is less than 90% of the established value.

Figure 4 shows a typical discharge waveform of a 1 A-5 ms pulse for a pair of tungsten needle-anode and tungsten plate-cathode electrodes in a CO_2 gas atmosphere. The electric current of rectangular waveform increases through the negative region at the beginning due to the property of the power supply circuit and it reaches to the set value within a 20 μs transition period. When the rectangular pulse current is set at 1 A, an arc discharge which does not depend on the electrode material or atmosphere occurs. Therefore the average discharge voltage (V_m) is lower than 60 V for this rectangular pulse, and this value is low enough to use the discharge energy effectively.

Table I Physical constants of electrode materials used for the microarc experiments and their physical properties.

TEST ELECTRODE	PURITY (%)	DENSITY ρ(g/cm²)	MELTING POINT Tm(℃)	THERMAL CONDUCTIVITY λ(cal/cm·s·℃)	SPECIFIC HEAT Cp(cal/g·℃)	THERMAL DIFFUSIVITY α(cm²/s)	HEAT IMPACT PARAMETER β(cm²·℃/s)	EVAPORATION HEAT A(J/g)	NOTE
1 W	99.95	19.24	3410	0.394	0.033	0.621	2118	4342	$\alpha=\lambda\cdot Cp^{-1}\cdot\rho^{-1}$
2 Ag	99.98	10.5	961	1.00	0.054	1.764	1695	2361	$\beta=\alpha\cdot Tm$
3 Cu	99.994	8.93	1083	0.94	0.092	1.142	1.237	4.819	
4 Ta	99.95	16.64	2996	0.13	0.034	0.230	689	4160	
5 Pt	99.98	21.45	1774	0.166	0.032	0.242	429	2621	
6 Zr	99.7	6.49	1852	0.05	0.069	0.112	207	6382	
7 Su	99.5	7.29	232	0.155	0.054	0.394	91	2454	
8 Be	99	1.84	1287	0.35	0.45	0.290	373	32741	
9 Ni	99.7	8.90	1453	0.22	0.105	0.206	299	6387	
10 Cr	99.9	7.19	1870	0.16	0.11	0.127	237	6712	
11 Fe	—	7.87	1809	0.18	0.11	0.156	282	—	
12 Zn	99.99	7.13	419	0.27	0.093	0.179	75	1730	
13 Mo	99.95	10.22	2620	0.34	0.061	0.212	555	6194	

2. 2 Discharge conditions

From the viewpoint of the reproducibility and the effective use of the discharge energy, the discharge conditions were decided as follows:

(1) The electrodes used for the discharge experiment are the pair of needle-anode and plate-cathode electrodes.

(2) CO_2 gas and air were used as the environment control gas, which were brown into the discharge gap, for the discharge experiment. This conditions was decided by the preparatory experiment.

2. 3. Selection of the test electrode material[2)]

Table I and Table II show the electrode materials used in this experiment and their typical physical properties. The materials listed in Table I are pure metals and the materials listed in Table II are refractory alloys and refractory thin film-coated metals.

Table II Compositions and production methods of test electrodes used for the microarc experiments.

TEST ELECTRODE	COMPOSITION	DESCRIPTION
1 W/CuW(SPRAY)	W (100~250 μm)	PLASMA SPRAY COATING ON CuW
2 W/CuW(CVD)	W (1 μm)	CVD COATING ON CuW
3 TiC/SUS(PVD)	Tic (20 μm)	PVD COATING ON SUS304
4 CuW	30Cu-W	NITTAN EME
5 HM-5	95.5W-CuNi	SUMITOMO HEAVY METAL
6 SUS304	18Cr-8Ni-Fe	AUSTENITIC STAINLESS STEEL
7 ALLOY302	30Cr-2Mo-Fe	FERRITIC STAINLESS STEEL
8 FA-5	1.9Ni-28.5Cr-45.6Fe-1.9Mo-5Al_2O_3	ALLOY K-63/Al_2O_3 CERMET

2. 4 Evaluation of the arc resistance for various electrode materials

Table III shows micro-arc test conditions for various pure matals and refractory materials, crater formation, effective haet flux, current density for 1 A-5 ms pulse in the CO_2 atmosphere. Tungsten, 95WFeNi (HM5) and TiC/SUS (TiC-thin-film-coated stainless steel) have the desiable arc resistance for pure metal, refractory alloy, and refractory thin-film-coated material, respectively. Craters were formed even on the high-meltingpoint metals after 5-7 pulse shots. However, especially for the materials with high thermal conductivity, the value of the discharge energy utility γ ($\gamma = E_r/E_p$, E_r = heat of evaporation of the crater, E_p = pulse energy) of the material which was evaluated from the size of a crater formed i. e., the amount of evaporation by the arc discharge, was small. The inverse number of the discharge energy utility γ^{-1} can be used as the energy dispersion factor, i. e. the larger the value of γ^{-1}, the harder to form a crater on the material.

Figure 5 shows the heat impact parameter $\beta (= \lambda T_m/\rho C_p$: λ = thermal conductivity, T_m = melting point, ρ = specific gravity and C_p = specific heat) and the energy dispersion factor γ^{-1} of pure metals listed in Table III in the air and the CO_2 atmospheres. Tung-

Table III Results for the arc-proof electrode materials evaluated in a CO_2 discharge.

TEST ELECTRODE (CATHDE)	PULSE CURRENT J-t (A-ms)	SHOT No. N (CYCLE)	SINGLE PULSE ENERGY ⟨Em⟩ (J)	TOTAL PULSE ENERGY EP (J)	PULSE VOLT. Vm (V)	CRATER SURFACE Sc ($10^{-5}cm^2$)	CRATER DEPTH f (μm)	EVAPORATION LOSS Wc (μg)	CRATER EVAPOLATION HEAT Er ($10^{-2}J$)	ENERGY USE γ (%)	HEAT FLUX Φ_{0ff} (kW/cm^2)	CURRENT DENSITY i (kA/cm^2)	FLASHOVER VOLTAGE ⟨VS⟩ (V)
1 W	1.03-5	7	0.118	0.827	41	0.00	0	0.00	—	—	5.22	127	640
2 Ag	1.03-5	7	0.112	0.728	43	159.36	6	10.04	2.23	2.85	2.70	0.63	514
3 Cu	1.03-5	7	0.152	1.065	42	70.65	15	9.46	4.56	4.28	5.95	1.42	1109
4 Ta	1.03-5	7	0.103	0.718	20	7.85	3	0.39	0.16	0.23	25.48	127	555
5 Pt	1.03-5	7	0.119	0.832	23	31.40	− 1	0.67	0.18	0.21	7.33	3.18	769
6 Zr	1.03-5	7	0.085	0.598	17	11.30	4	0.29	0.19	0.31	15.04	8.85	795
7 Sn	1.03-5	7	0.091	0.638	18	70.65	30	15.45	3.79	0.59	2.55	1.42	621
8 Be	1.03-5	7	0.133	0.930	26	70.65	9	1.17	3.83	4.12	3.68	1.42	1084
9 Ni	1.03-5	7	0.114	0.797	22	13.27	17	2.01	1.28	1.61	16.58	7.53	682
10 Cr	1.03-5	7	0.107	0.749	21	9.50	14	0.96	0.64	0.86	22.11	10.53	774
11 Fe	1.03-5	7	0.080	0.563	16	41.53	7	2.29	—	—	3.85	2.41	385
12 Zn	1.03-5	7	0.130	0.907	25	28.34	23	4.65	0.80	0.89	8.82	3.53	921
13 Mo	1.03-5	7	0.135	0.947	26	11.30	3	0.35	0.21	0.23	23.01	8.84	1232
14 Fa5	1.03-5	7	0.084	0.585	16	57.23	2	0.86	—	—	2.80	1.75	897
15 HM5	1.03-5	7	0.121	0.848	24	7.85	3	0.45	0.19	0.23	30.57	127	370
16 W/CuW(SPRAY)	1.03-5	7	0.128	0.899	25	9.50	17	3.07	1.33	1.48	26.32	10.53	834
17 W/CuW(CVD)	1.03-5	7	0.129	0.904	25	7.85	19	2.83	1.23	1.36	31.85	127	846
18 ALLOY302	1.03-5	7	0.085	0.597	17	80.07	3	1.85	—	—	2.12	1.25	471
19 SUS304	1.03-5	7	0.073	0.511	14	22.69	10	1.80	—	—	6.17	4.41	631
20 Cuw	1.03-5	7	0.122	0.856	24	20.39	13	4.28	—	—	11.77	4.90	428
21 TiC/SUS(PVD)	1.03-5	7	0.093	0.648	18	5.02	2	0.05	—	—	35.86	19.92	970

0.25 mmϕW NEEDLE(+) vs PLATE ELECTRODE(−), GAP=0.1 mm, CO_2(760 Torr/23±1℃),

Vm=Ep/t-J, Wc=f-Sc-ρ, Er=Wc-A, γ=Er/Ep, Φ_{0ff}=0.1 Vm-J/Sc, i=J/Sc

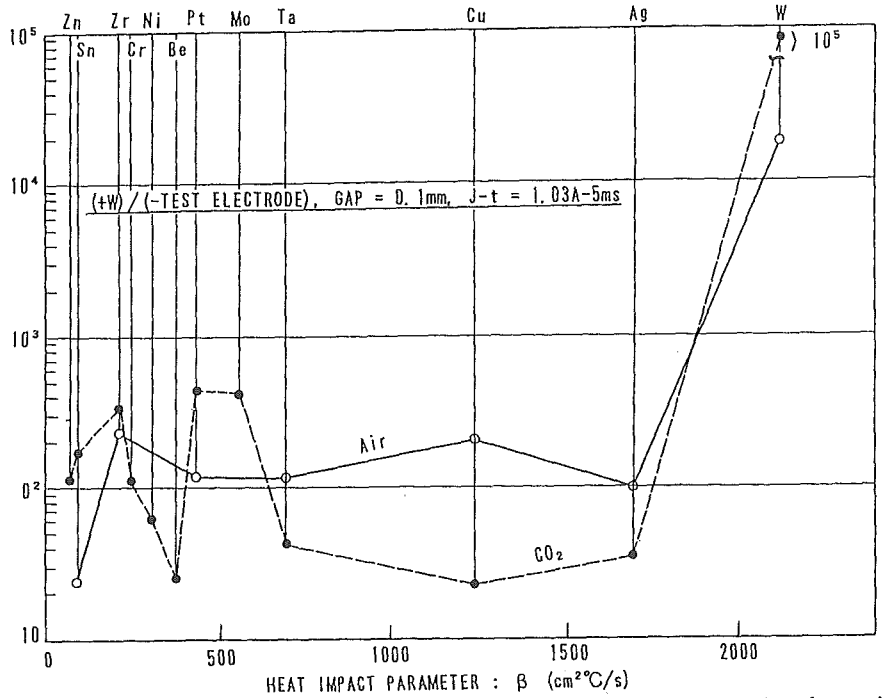

Fig. 5 The relation between heat impact parameter and the energy dispersion factor in the normal-air and the CO_2 atmospheres for various metal electrode materials.

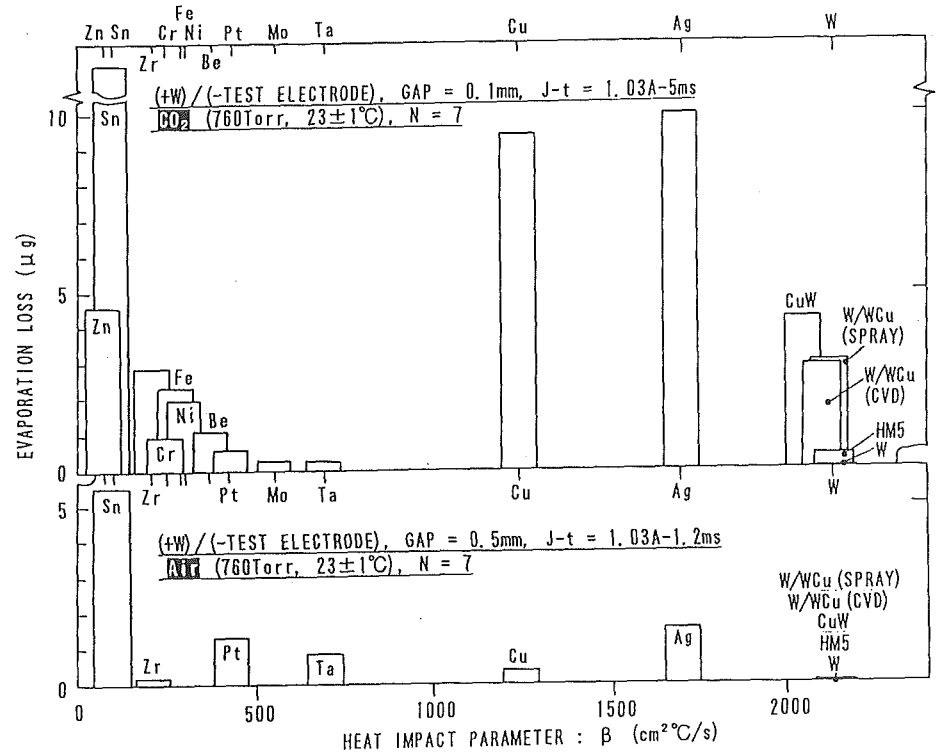

Fig. 6 Evaporation losses of various electrode materials by the discharge in the normal-air and CO_2 atmospheres.

sten has the highest value of γ^{-1} in the CO_2 atmosphere. Besides the tungsten electrode, molybdenum, platinum and zirconium have excellent arc resistances because they have much higher value of γ^{-1} than other materials in Fig. 5.

Figure 6 shows the relation between crater formation and heat impact parameter β in the air and CO_2 gas atmosphere. The crater formation for typical electrode mate-

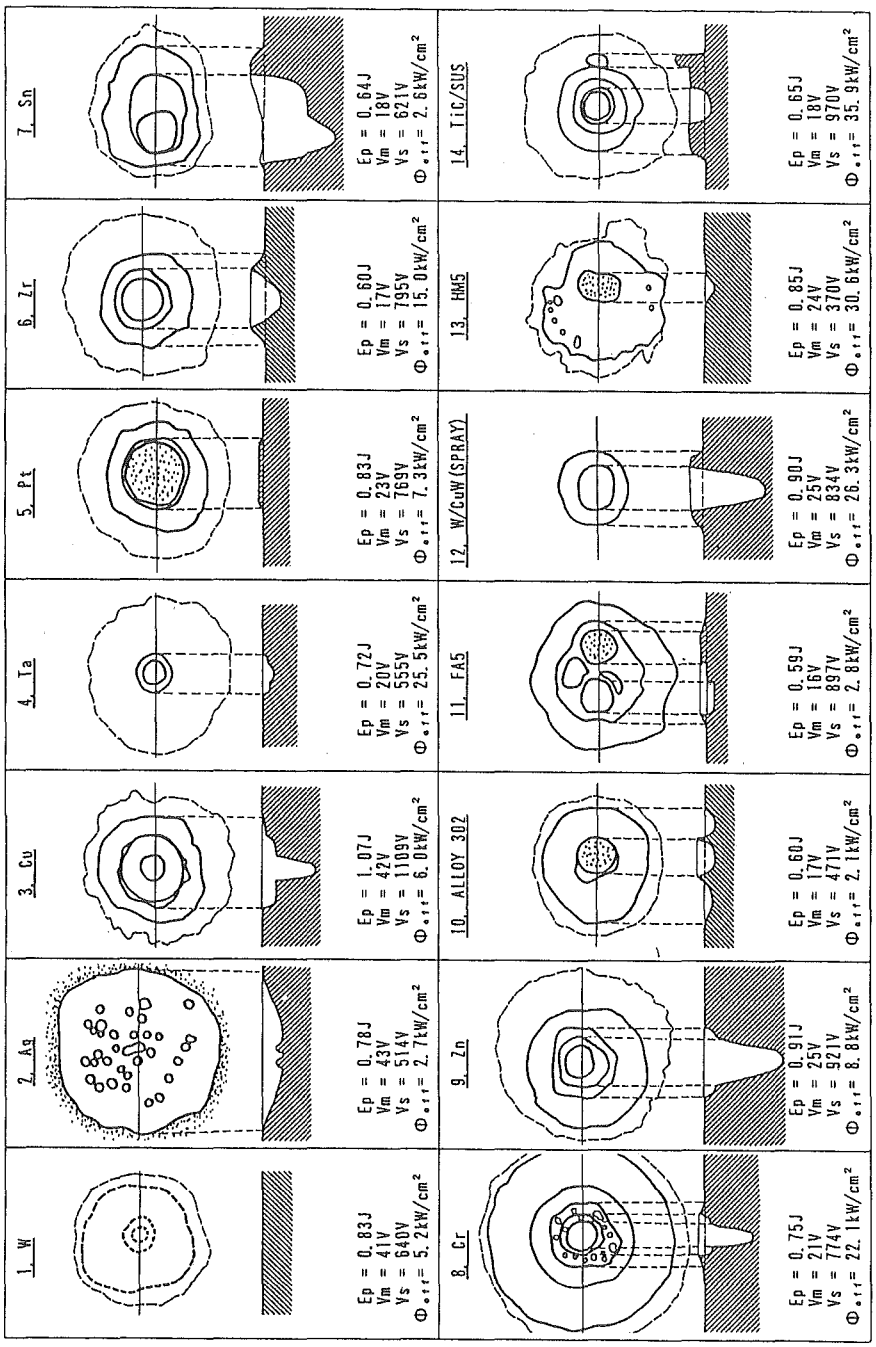

Fig. 7 The crater formation for typical electrode materials in CO_2 atmosphere.

rials is shown in Fig. 7. For the copper and silver material, the amount of the evaporation wear in CO_2 is particularly large, however, high purity tungsten has excellent arc resistance in both atmospheres. Although the thin-film tungsten coated electrodes produced by plasma spraying method and the CVD coating process and HM5 also have excellent arc resistance in the air, the evaporation in CO_2 atmosphere was large. For pure metal electrode materials, the evaporation wear of tantalum, molybdenum and platinum in the CO_2 atmosphere and that of zirconium and copper in the air atmosphere was also small. The crater formation for pure metals except for Zr, Cu, and Ag showed a tendency to be reduced as the increase of the heat impact parameter β and did not depend on the discharge environment. High purity tungsten has a maximum β value among the electrode materials tested and this means that tungsten has the best arc resistance.

3. Electrode Splash Experiment[3,4]

3. 1 Refractory thin-film-coated electrode structure

The electrode splash experiment was carried out by using the TiC- and TiN-thin-film-coated stainless electrodes produced by the PVD method to investigate the performance of the electrodes, the observation of the current phenomena and the electrode wear under the coal-combustion condition. The film-coated electrodes were produced by following procedure; First, as described in Fig. 8, the 0.5 μm titanium buffer layer was produced on the SUS304 substratum by the hollow-cathode-discharge-vaporization method. Then, 6~20 μm TiC (TiN) film was produced on the Ti layer. These electrodes are produced assuming that the operating temperature is lower than 400℃ at the electrode surface.

3. 2 Experiment using TiC/SUS electrodes

A short-term electrode splash experiment was carried out under the oxygen-rich

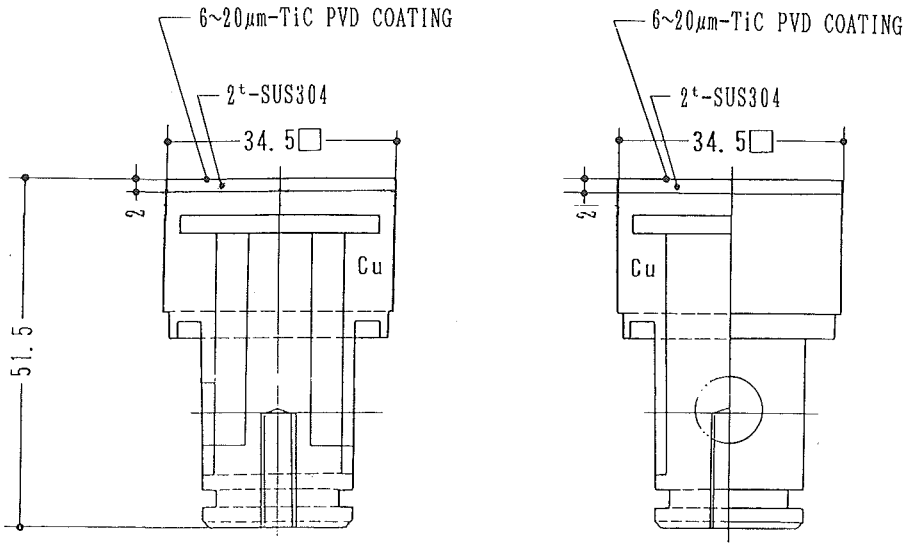

Fig. 8 TiC-coated electrode prepared by PVD.

(Fuel/O_2=0.95) COM (Coal Oil Mixture) combustion condition. This condition simulates the practical operation of coal-combustion MHD generator. Figure 9(a) show the equipment used for this experiment. In Figure 9(b), the potential probe is placed at the midpoint between the ring electrode and the test electrode and can be used to measure the electrode voltage drop and the slag impedance.

Figure 10 shows a typical time dependence of the combustor heat input, the heat flux, the electric current, the applied voltage (V_{ac}) between the test electrode and the ring electrode, and the voltage drop (V_p) measured between the probe and the test electrode during a splash experiment. A solid slag layer of about 1.5 mm thickness is formed to the electrode surface before the current flows and the liquid slag flows con-

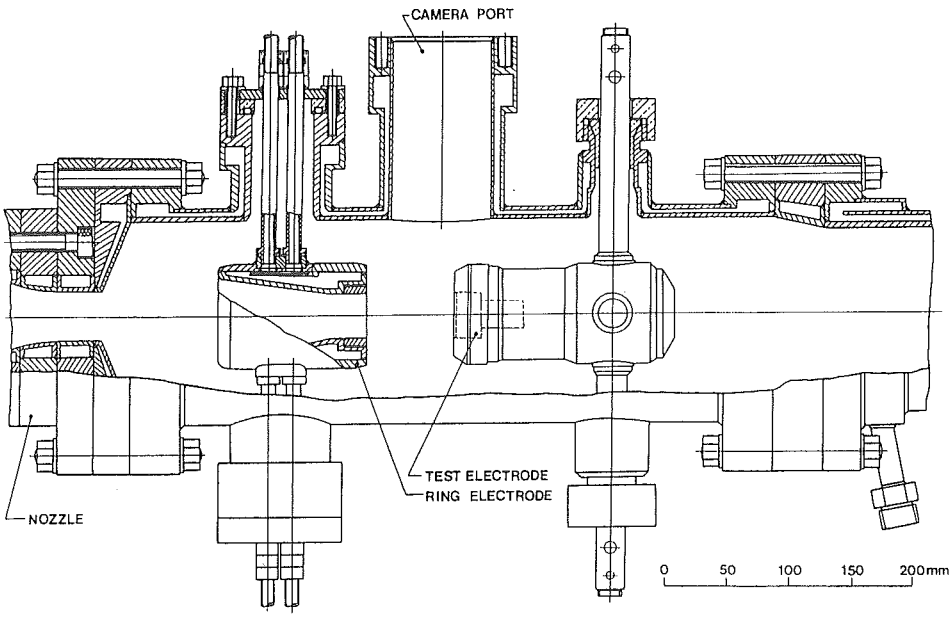

Fig. 9(a) Equipment for the splash experiment.

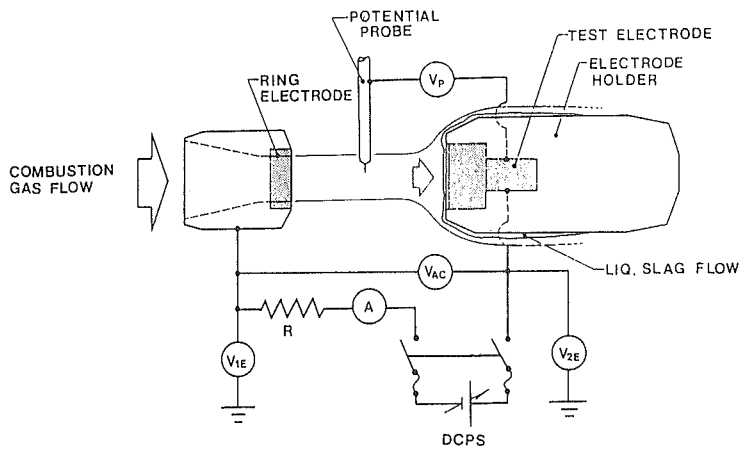

Fig. 9(b) A measuring circuit for volt-ampere characteristics of discharge.

stantly on the solid slag layer. When the current flows, several big arcs appear on the slag layer. These big arcs melt the adhesion of the slag, and makes it flow out. Then the constant microarc discharge occurs. Because of these phenomena, the heat flux by the current becomes large. This is observed more clearly for Tic-coated electrode than for other metal electrode. Also, from a viewpoint of the voltage-current characteristics, a steep rise in the current to the applied voltage and a high anode-electrode voltage drop (V_p) are observed for Tic-coated electrode. Figure 11 clearly shows this characteristics, particularly in the low current density region. The difference in slag adhesion conditions for various electrode materials and arc modes depend on the wettability of the slag on the electrode surface.

Table IV shows the combustion conditions, the type of electrode, the operation parameters, the weight losses and the surface state of the electrode after the experiments. A 15 wt% Horonai-coal mixed into diesel-oil was used as the COM fuel. The lower column of the same table shows the chemical composition (mol%) of the slag formed by the COM combustion.

Figure 12 shows the average value of the wear of TiC-coated SUS electrode compared to the various pure metal and alloy electrodes. It is observed that TiC-coated SUS electrode has the best arc resistance among the electrodes shown in Fig. 12. However, the difference of the amount of the electrode wear by the current density of 1.03 A/cm^2 between TiC-coated SUS and other materials is not so large. Also, the difference of the wear of TiC-coated SUS electrode by the change of the current density is small. This means that the oxidation of TiC, i.e. the formation of TiO_2, is

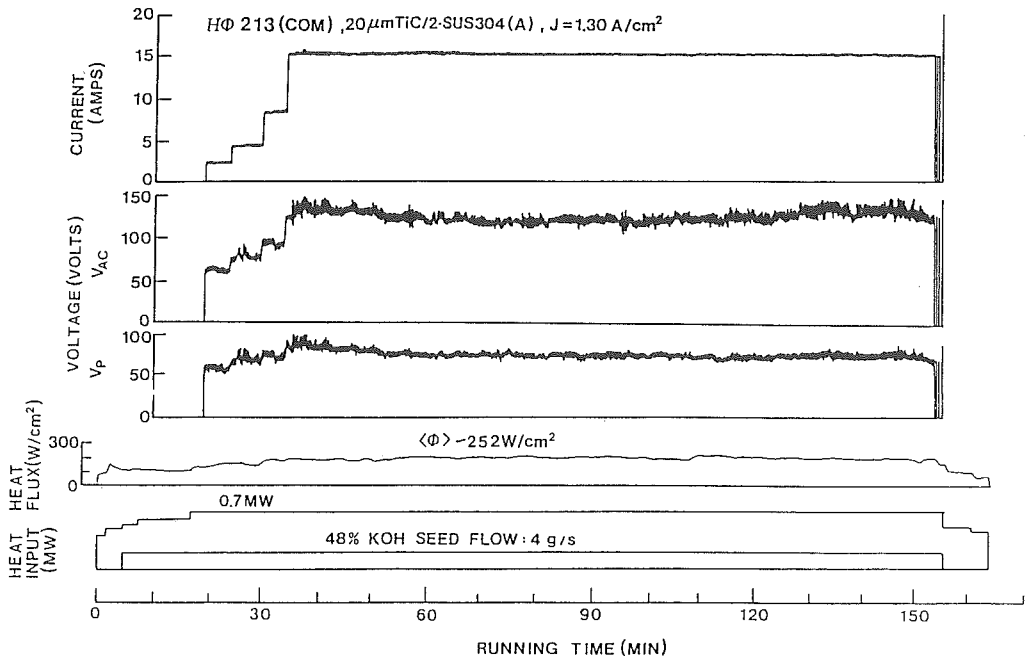

Fig. 10 The relation between running time and the combustor heat input in a splash experiment, the electrode heat flux, the electric current, the voltage (V_{ac}) between the test electrode and a ring electrode, and the voltage (V_p) between the probe and the test electrode.

Table IV Splash test results for TiC and W electrodes.

RUN	ELECTRODE	SLAG	HEAT INPUT (MW)	DURATION (MIN)	HEAT FLUX (W/cm^2)	CURRENT DENSITY (A/cm^2)	ELECTRODE DROP (V)	ELECTRODE WEAR ($\mu g/C$)	REMARKS
198	6 μm-TiC/2-SUS	HCS	0.7	144	233	1.30	44	1.4	EXCELLENT
199	6 μm-TiC/2-SUS	HCS	0.7	168	230	1.30	45	5.4	OXIDE FORMATION
200	3 μm-TiN/0.5-SUS	HCS	0.7	150	202	0.82	52	4.0	LOCALLY MELTING
206	6 μm-TiC/2-SUS	HCS+C	0.7	165	271	1.30	26	7.3	OXIDE FORMATION
210	2-SUS304	HCS	0.7	164	234	1.30	58	6.2	EXCELLENT
211	20 μm-TiC/2-SUS	HCS	0.7	87	240	1.30	100	0.6	ARC DEGRADATION
212	20 μm-TiC/2-SUS	HCS	0.7	154	205	0.52	70	4.8	ARC DEGRADATION
213	20 μm-TiC/2-SUS	HCS	0.7	164	252	1.30	75	6.5	ARC DEGRADATION
214	20 μm-TiC/2-SUS*	HCS	0.7	175	227	1.30	72	9.2	ARC DEGRADATION
215	20 μm-TiC/2-SUS*	HCS	0.7	169	206	1.30	80	7.5	ARC DEGRADATION

HCS SLAG: SiO_2=32.8, Al_2O_3=20.1, Fe_2O_3=3.03, CaO=3.16, MgO=0.81, TiO_2=0.72, Na_2O=0.65, K_2O=38.6 (mol%)

HCS+C SLAG: 27.6 13.8 4.45 19.0 3.01 0.59 0.75 30.5

* 600℃-30MIN HEAT TREATMENT IN AIR

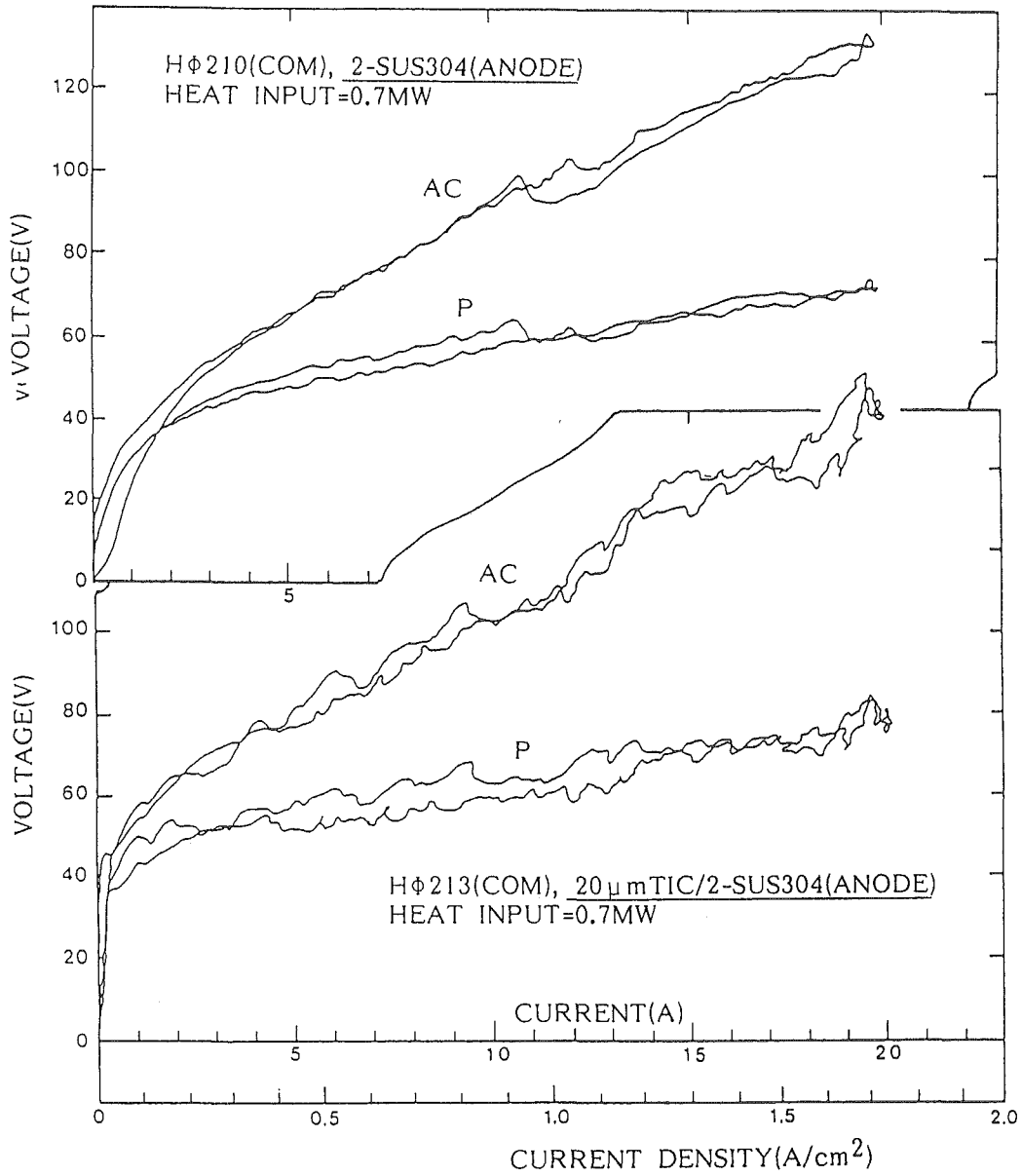

Fig. 11 The voltage-current characteristics between the test electrode and a ring electrode (AC) and between the probe and the test electrode (P). The test electrodes are TiC-coated and non-coated stainless steel cold-type slagging electrodes.

occurred at relatively low temperatures on the electrode surface during the experiment. As listed in Table IV, the electrode wear in RUN214 and RUN215 is lager than other RUNs. The TiC-coated electrodes used in these two RUNs were treated with heat at 600℃ for 30 minutes in an oxidized atmosphere before the experiment. The insulation resistance at the surface of these heat-treated electrodes was several orders higher than before the heat-treating. This clearly suggested that TiO_2 is formed on the surface of the electrodes. TiO_2 has low melting point and acts as an electrical insulator. There-

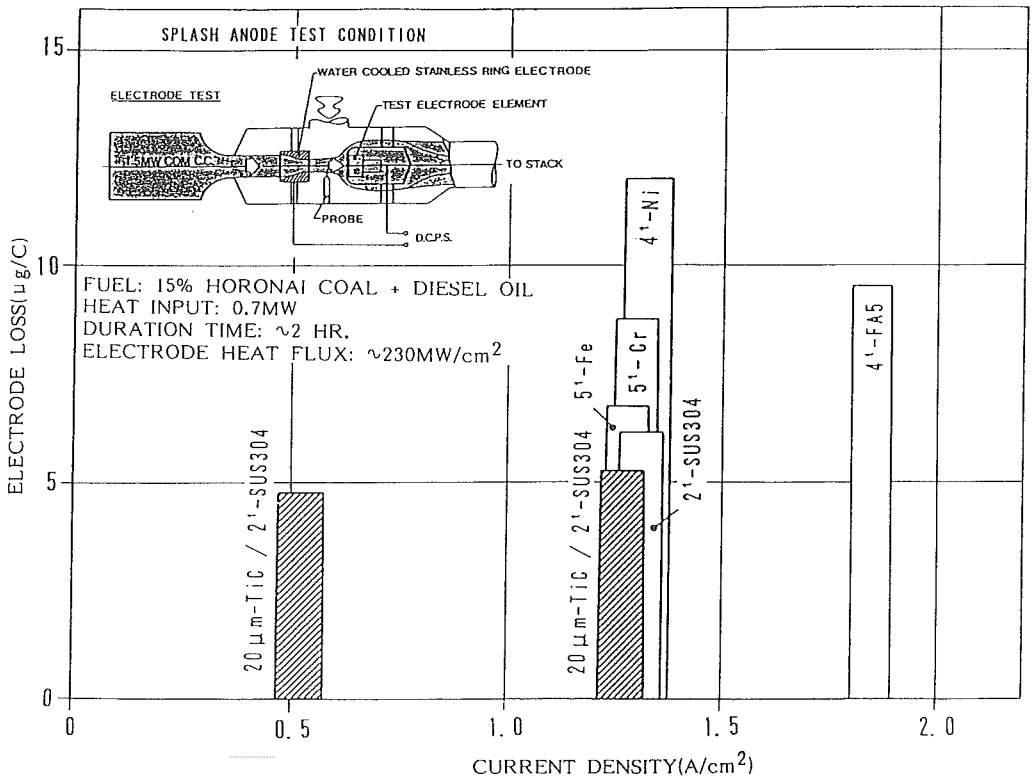

Fig. 12 The average wear of TiC electrodes with a current density of 1.3 A/cm² as compared with the various pure metal and alloy electrodes.

fore, electric breakdown of TiO_2 by the arc discharge occurred and accelerated the electrode wear with the melting or evaporation of the TiC surface.

The same experiments for tungsten system electrodes are proceeding at present.

4. Conclusions

In order to evaluate the arc resistance of the electrode materials for an MHD generator, the discharge experiment and splash experiment were carried out. The following conclusions were obtained:

1) In CO_2 environment, tungsten, tungsten-based alloy, tantalum, molybdenum, platinum and TiC-coated stainless steel have the desirable arc resistance.

2) In the splash experiment, TiC-coated stainless steel electrode has more desirable arc resistance than the electrode without TiC layer.

References

1) T. Okuo, Y. Kusaka, T. Takano, and K. Kato: "Electrode Developmentand Testing for Coal-Fired MHD Generator", 26th SEAM

2) T. Okuo: "Experimental Studies on Channel Walls for Magnetohydrodynamic(MHD) Electrical Power Generation" Researches of the ETL, No. 874 (1986)

3) T. Okuo: "Electrode Phenomena in COM Combustion Splash Flow Gas Plasma (1)", Journal of

High Temperature Society, Vol. 14, No. 13 (1987)
4) T. Okuo : " Electrode Phenomena in COM Combusion Splash Flow Gas Plasma (2) ", Journal of High Temperature Society, Vol. 14, No. 1 (1988)